JOURNAL OF MAGNETIC RESONANCE **133,** 123–128 (1998)
ARTICLE NO. MN981446

Five-Quantum Coherence of $I = \frac{5}{2}$ Nuclei: ^{27}Al in an Al_2O_3 Single Crystal

A. Kaikkonen, E. E. Ylinen, and M. Punkkinen

Wihuri Physical Laboratory, Department of Physics, University of Turku, Turku FIN-20014, Finland

Received May 7, 1997; revised March 20, 1998

Optimal conditions were calculated for excitation and detection of the five-quantum coherence of quadrupolar nuclei with $I = \frac{5}{2}$ in single crystals, observed by the two-pulse sequence $(\theta_1)_x - \tau_1 - (\theta_2)_\alpha - \tau_2$, where α is the phase cycling angle. Variations in the pulse lengths, the relative values of the nutation frequency $\omega_1 = \gamma B_1$, and the quadrupolar frequency ω_Q as well as in the resonance offset were taken into account. In addition, the effect of the pulse length on the intensity of spectral lines was considered. Theoretical results were compared with experiments on ^{27}Al nuclei in an Al_2O_3 single crystal. © 1998 Academic Press

Key Words: **Five-quantum coherence; ^{27}Al NMR; Al_2O_3 single crystal.**

INTRODUCTION

The first observation of multiquantum coherence was made in 1959 by a continuous wave method (*1*). With the development of computer technology new methods, for example Fourier transform spectroscopy and two-dimensional NMR, were introduced (*2*). These opened new prospects for the observation of the multiquantum coherences via various coherence transfer methods. Although a substantial percentage of recent publications concentrate on the development and application of these methods on liquids, there is a fair amount of interest also in liquid crystals and solids. In particular, plenty of experimental work has been done on quadrupolar nuclei with $I = 1$ and $\frac{3}{2}$ (*3–8*). When the maximum order ($2I$) coherence or any of the coherences $-m \leftrightarrow +m$ is excited, the first order correction due to the quadrupole coupling does not cause any broadening. However the second order correction broadens even these coherences in powder samples. The broadening can be averaged out by different sample rotation techniques, for example, dynamic angle spinning (DAS) or double rotation (DOR) (*9–11*).

Recently a new method for high-resolution experiments in quadrupolar solids was introduced by combining multiquantum coherence methods with magic angle sample rotation (*12, 13*). Such experiments are now possible with normal NMR spectrometers and MAS accessories (*14–20*). Nevertheless, this method suffers from the same disadvantage as other multiquantum experiments: the multiquantum excitation and the subsequent conversion to the single-quantum (1Q) coherence become less efficient when the quadrupole coupling increases (*13, 14*).

Here we concentrate on nuclei with the spin $I = \frac{5}{2}$, although some computations are also done for spins $\frac{3}{2}$, $\frac{7}{2}$, and $\frac{9}{2}$. The efficiency of the excitation and conversion of the $2I$ multiquantum coherence is studied for a single crystal. This maximal order of coherence is chosen because it demonstrates most clearly the effect of the offset and chemical shift. Besides, there is only one such transition while for example the three-quantum (3Q) coherence $-\frac{3}{2} \leftrightarrow +\frac{3}{2}$, which is also unshifted by the first order quadrupole correction, might be disturbed by others 3Q coherences. Both the excitation and conversion are accomplished by one rectangular RF pulse each. Thus our pulse sequence consists of two pulses with the phase of the second pulse incremented in steps of 30° (in the case of the five quantum (5Q) coherence of $I = \frac{5}{2}$ nuclei). The coherence transfer pathway could have been selected also by pulsed field gradients but this method suffers still from a rather low sensitivity (*21–24*). Optimal pulse lengths and ratios ω_1/ω_Q ($\omega_1 = \gamma B_1$ and ω_Q is the quadrupolar frequency) are found for the maximal excitation and conversion efficiency. The efficiency is compared with that of a weak RF irradiation at the exact resonance $\omega_0 = \gamma B_0$. Also the influence of the resonance offset is studied. Amoureux *et al.* (*14*) have recently made similar calculations.

Because of the relatively high value of the ω_1/ω_Q required for observing a sufficiently strong signal from the 5Q coherence, a sample with a low ω_Q was chosen. We used a single crystal of Al_2O_3 in our experiments. It has the maximum ^{27}Al quadrupolar frequency equal to 179.5 kHz (*25*). By calculating Fourier transforms of the acquired induction-decay-like signals after the phase-incremented two-pulse sequences and by gradually changing the evolution time between the pulses it was possible to obtain information about the 5Q coherence and test our computations.

1090-7807/98 $25.00

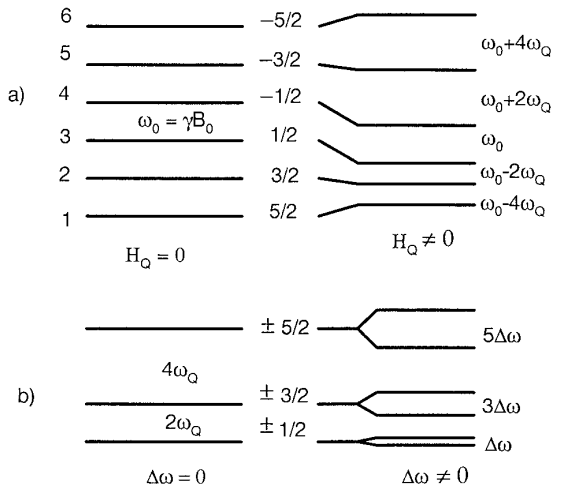

FIG. 1. Energy levels and resonance frequencies of $I = \frac{5}{2}$ nuclei in (a) laboratory and (b) rotating frames.

THEORY

We consider nuclei with the spin $I = \frac{5}{2}$ in a solid, interacting with the external static magnetic field $\mathbf{B}_0$ and with the electric field gradient at the nuclear site. The homonuclear dipolar interactions and the second order quadrupolar interactions are not taken into account. The energy levels in the laboratory and rotating frames are shown in Fig. 1.

In the coordinate frame rotating at the spectrometer frequency ω_r the Hamiltonian without the multiplier $\hbar$ becomes

$$H_Q = \Delta\omega I_z + (\omega_Q/3)[3I_z^2 - I^2]. \qquad [1]$$

Here I_z and I are spin operators, $\Delta\omega = \omega_r - \omega_0 = \omega_r - \gamma B_0$ is the resonance offset, and

$$\omega_Q = (3\cos^2\theta - 1 + \eta\sin^2\theta\cos 2\phi)3e^2qQ/80\hbar. \qquad [2]$$

In Eq. [2], e^2qQ is the quadrupolar coupling constant, η is the asymmetry parameter, and θ and ϕ are the polar angles of $\mathbf{B}_0$ in the principal axes frame of the quadrupole coupling. When an RF field at the frequency ω_r is applied, Eq. [1] is replaced by the Hamiltonian

$$H_r = \Delta\omega I_z + \omega_Q[3I_z^2 - I(I+1)]/3 - \omega_1(I_x\cos\alpha + I_y\sin\alpha). \qquad [3]$$

Here α determines the phase of the RF field and it is the angle which is incremented in phase cycling.

The effect of H_r can be worked out more easily by using the single-transition operators $I_\beta^{(ij)}$ ($\beta = x, y, z$; $i, j = 1, 2, \ldots, 6$), introduced by Wokaun and Ernst (*26*) and Vega (*27*). The Hamiltonian H_r can then be written as

$$\begin{aligned} H_r = {} & (5\Delta\omega + 20\omega_Q/3)I_z^{(16)} + (3\Delta\omega - 4\omega_Q/3)I_z^{(15)} \\ & + (\Delta\omega - 16\omega_Q/3)I_z^{(14)} + (-\Delta\omega - 16\omega_Q/3)I_z^{(13)} \\ & + (-3\Delta\omega - 4\omega_Q/3)I_z^{(12)} \\ & - \sqrt{5}\,\omega_1[(I_x^{(12)} + I_x^{(56)})\cos\alpha + (I_y^{(12)} + I_y^{(56)})\sin\alpha] \\ & - \sqrt{8}\,\omega_1[(I_x^{(23)} + I_x^{(45)})\cos\alpha + (I_y^{(23)} + I_y^{(45)})\sin\alpha] \\ & - 3\omega_1[I_x^{(34)}\cos\alpha + I_y^{(34)}\sin\alpha]. \end{aligned} \qquad [4]$$

Initially the system is assumed to be at thermal equilibrium. The corresponding density matrix, without the temperature-independent constant term, can be written

$$\rho_0 = bI_z = b(5I_z^{(16)} + 3I_z^{(15)} + I_z^{(14)} - I_z^{(13)} - 3I_z^{(12)}) \qquad [5]$$

with $b = \omega_0/[(2I+1)kT]$. In order to calculate the effect of a single rectangular pulse on the spin system it is necessary to diagonalize the Hamiltonian [4]. This can be done by replacing the single-transition operators and H_r by 6×6 matrices and by finding the matrix T, which diagonalizes H_r,

$$H_r^t = T^{-1}H_rT. \qquad [6]$$

Actually the T matrix is constructed from the eigenvectors of H_r. The density matrix ρ_0 has to be transformed simultaneously $\rho_0^t = T^{-1}\rho_0 T$. Because H_r^t does not depend on time the evolution of $\rho(t)^t$ is obtained from the expression

$$\rho(t)^t = \exp\left(-\frac{i}{\hbar}tH_r^t\right)\rho_0^t\exp\left(\frac{i}{\hbar}tH_r^t\right). \qquad [7]$$

There are five linearly independent $I_z^{(ik)}$ operators in H_r^t. However, because the commutator $[I_p^{(ij)}, I_z^{(ik)} + I_z^{(jk)}]$ vanishes for $p = x$ or y and because the operators belonging to the same transition obey the cyclic commutation relations $[I_l^{(ik)}, I_m^{(ik)}] = iI_n^{(ik)}$, it is reasonable to express H_r^t in terms of cyclically commuting operators including linearly dependent $I_z^{(ik)}$. For example when one considers the effect of the diagonalized Hamiltonian H_r^t on the term $I_x^{(56)}$ in the transformed density matrix, the Hamiltonian

$$H_r^t = c_{12}^z I_z^{(12)} + c_{13}^z I_z^{(13)} + c_{14}^z I_z^{(14)} + c_{15}^z I_z^{(15)} + c_{16}^z I_z^{(16)}$$

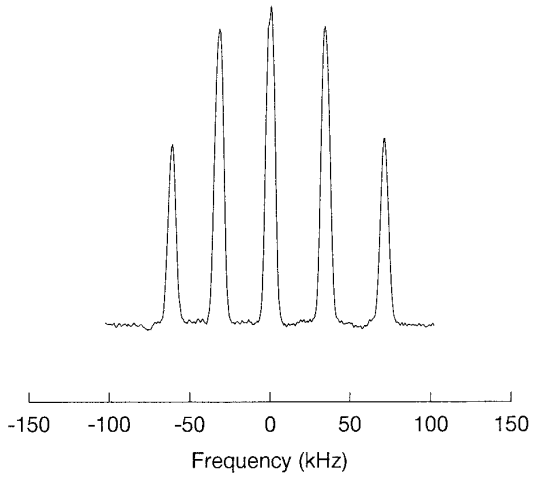

FIG. 2. ^{27}Al spectrum in an Al_2O_3 single crystal with $\nu_Q = 15.7$ kHz, measured at $\nu_0 = 52.1$ MHz.

is rewritten as

$$H_r^t = c_{12}^z I_z^{(12)} + c_{13}^z I_z^{(13)} + c_{14}^z I_z^{(14)} + \frac{1}{2}(c_{15}^z + c_{16}^z)(I_z^{(15)} + I_z^{(16)}) + \frac{1}{2}(c_{16}^z - c_{15}^z) I_z^{(56)}. \quad [8]$$

Here the coefficients c_{1i} are equal to the diagonal matrix elements $(H_r^t)_{ii}$. Since $I_x^{(56)}$ and $I_z^{(15)} + I_z^{(16)}$ commute, only the last term of Eq. [8] is relevant and we obtain

$$\exp(-itH_r^t) I_x^{(56)} \exp(itH_r^t) = I_x^{(56)} \cos\left[(c_{16}^z - c_{15}^z)\frac{t}{2}\right] + I_y^{(56)} \sin\left[(c_{16}^z - c_{15}^z)\frac{t}{2}\right]. \quad [9]$$

After a similar procedure is completed for all the terms of ρ_0^t, the entire density matrix has to be transformed back into the rotating frame by the inverse transformation $\rho(t) = T\rho^t(t)T^{-1}$.

Then the evolution during the time between the pulses is calculated. This corresponds to a simple rotation around the z axes in the 15 subspaces $\{I_x^{(ik)}, I_y^{(ik)}, I_z^{(ik)}\}$ with the angular frequencies $\omega_{ik} = (H_Q)_{ii} - (H_Q)_{kk}$. The evolution of the density matrix during the second pulse is solved by repeating the steps [6]–[9]. This method can in principle be applied to calculate the response of the system consisting of any finite number of energy levels after a finite number of pulses.

In order to transform the 5Q coherence into an observable single-quantum coherence we applied the second pulse $(\theta_2)_\alpha$. The phase of this pulse, α, was incremented in steps of 30°, while the reference phase was simultaneously changed in steps of 180°. The phase of the first pulse was kept unchanged. Thus a total of 12 phase-cycled sequences were needed to select the 5Q coherence from the various coherences between the pulses. This procedure automatically restricts the change of the coherence order during the second pulse to ± 6, or from the coherence ± 5 to the coherence ∓ 1. Moreover, when we set the RF pulse on the center of the spectrum, the x component of the acquired signal vanishes, which allows for easy tuning of the phase of the receiver.

The algorithm described above and the ''Maple'' programming package were employed in order to calculate the response of the system on the two-pulse sequences with the described phase cycling as functions of the pulse lengths, the ratio ω_1/ω_Q and the resonance offset.

EXPERIMENTAL

Experiments were carried out by using the Bruker MSL 300 pulsed NMR spectrometer, operated at the ^{27}Al resonance frequency 52.1 MHz at room temperature. The Al_2O_3 single crystal was oriented relative to $\mathbf{B}_0$ in such a way that the splitting between the neighboring lines in the five-line spectrum was equal to $2\nu_Q = 2\omega_Q/2\pi = 31.4$ kHz (Fig. 2). This corresponds to the value of ω_Q in Eq. [2] equal to 98.6×10^3 rad/s. The RF field was calibrated by the proton NMR signal from a rubber sample, measured at the same resonance frequency but at a lower field. An independent calibration was obtained from the ^{27}Al signal after orienting the Al_2O_3 crystal in such a way that all the lines collapsed into a single one. The results of these two methods agreed quite well with each other. The spin–lattice relaxation time T_1 was observed to be 130 s for all lines. Unfortunately, because of the long relaxation time and low signal/noise ratio an acquisition time of 3 h was needed to determine one experimental point.

RESULTS AND DISCUSSION

We used the algorithm explained above to calculate the variation of the amplitude of the 5Q coherence, excited by one

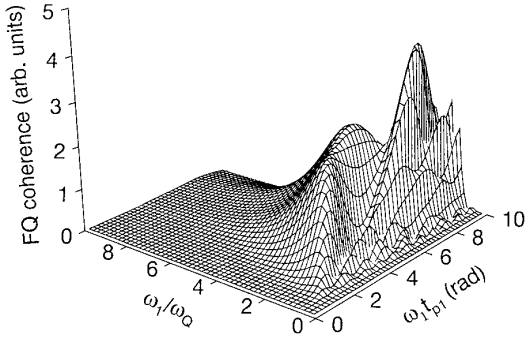

FIG. 3. Amplitude of the FQ coherence after one resonant pulse as functions of ω_1/ω_Q and $\omega_1 t_{p1}$.

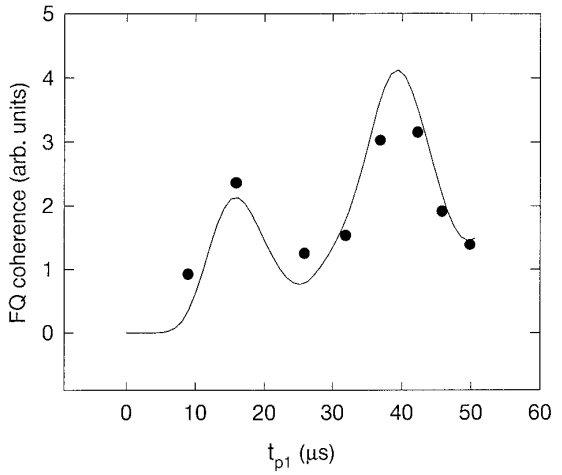

FIG. 4. Amplitude of the ^{27}Al FQ coherence after one pulse versus t_{p1} in an Al_2O_3 single crystal, observed after phase-cycled two-pulse sequences. $t_{p2} = 14$ μs, $\omega_1 t_{p2} = 2.6$, $\tau_1 = 10$ μs, $\omega_Q/2\pi = 15.7$ kHz, and $\omega_1/\omega_Q = 2.0$ for both pulses.

rectangular pulse at the frequency $\nu_0 = \gamma B_0/2\pi$, with $\omega_1 t_{p1}$ and ω_1/ω_Q. The results are shown in Fig. 3, where the variable $\omega_1 t_{p1}$ is restricted to 10 corresponding roughly to the highest B_1 field and the longest pulse which could safely be used. The maximum is achieved when $\omega_1/\omega_Q = 2.0$ and $\omega_1 t_{p1} = 8.0$. To compare the intensities shown in Fig. 3 with experiments, we used the two-pulse sequence $(\theta_1)_x - \tau_1 - (\theta_2)_\alpha - \tau_2$, where the phase-cycled second pulse transforms the 5Q coherence into the observable 1Q coherence. Fourier transforms of the acquired signals were calculated relative to τ_2 and the amplitude of the central line of the spectrum was taken as the measure of the 5Q coherence.

Figure 4 shows the variation of the ^{27}Al 5Q coherence amplitude with the pulse length t_{p1} in the single crystal of Al_2O_3, oriented as explained above, at room temperature. The ratio ω_1/ω_Q was equal to 2.0 for both the pulses, while the length of the second pulse was chosen to fulfill $\omega_1 t_{p2} = 2.6$. The continuous curve represents the cross section of Fig. 3 for $\omega_1/\omega_Q = 2.0$. The agreement between theory and experiment is fair. Our results agree also with the calculations of Amoureux *et al.* (*14*).

It is also possible to excite multiquantum coherences by a weak irradiation. For the amplitude of the *y* component of the 5Q coherence c_{16}^y Yatsiv (*1*) derived the expression

$$c_{16}^y(t_{p1}) = 5b \sin[k_{5/2}(\omega_1/\omega_Q)^4 \omega_1 t_{p1}] \qquad [10]$$

provided the nuclei ($I = \frac{5}{2}$) are originally at thermal equilibrium and $\omega_1/\omega_Q \ll 1$. Here t_{p1} is the duration of the irradiation and $k_{5/2}$ is a numerical factor. The term $k_{5/2}(\omega_1^5/\omega_Q^4)$ can be considered as an effective RF field B_1^{eff} multiplied by γ. We calculated the response of the spin system to such an irradiation and obtained the same result with the coefficient $k_{5/2}$ equal to 0.013. The small $k_{5/2}$ value and the requirement $\omega_1/\omega_Q \ll 1$ mean that very long irradiation times are needed to make $\gamma B_1^{\text{eff}} t_{p1} = \pi/2$. Quite easily t_{p1} becomes longer than the relaxation time.

Such a behavior is even more pronounced with nuclei having larger I values. According to our calculations the coefficients k_I are $k_{7/2} = 1.52 \times 10^{-4}$ and $k_{9/2} = 8.72 \times 10^{-7}$. The corresponding effective fields are then $k_{7/2}(\omega_1^7/\omega_Q^6)$ and $k_{9/2}(\omega_1^9/\omega_Q^8)$ for the spins $\frac{7}{2}$ and $\frac{9}{2}$, respectively. Therefore a weak irradiation is not as effective as one hard pulse in exciting the 5Q coherence although the maximum amplitude of Eq. [10] for $I = \frac{5}{2}$ is 20% larger than the maximum in Fig. 3 corresponding to $\omega_1 t_{p1} = 8.0$ and $\omega_1/\omega_Q = 2.0$. A similar picture is obtained for spins $\frac{3}{2}$, $\frac{7}{2}$, and $\frac{9}{2}$. However, the value of ω_1/ω_Q corresponding to the maximum excitation efficiency of the 2I coherence increases with I and is 1.4, 3.4, and 4.8 for the mentioned spins, respectively.

The amount of the 5Q coherence transformed into the observable 1Q coherence depends, obviously, on the length of the second pulse. Therefore it is necessary to find also the optimal length for the second pulse while keeping the first pulse optimized as explained above. Our calculations on the efficiency of the coherence transfer from the highest order to 1Q show, in agreement with previous studies (*13, 26*), that ω_1 should be as high as possible for the maximum efficiency. However, in our experiment both pulses had the same B_1 field, because it was close to the highest possible value for the ''fifth'' channel of our spectrometer. Figure 5 represents the amplitude of the 1Q signal, proportional to the 5Q coherence between the pulses, after the second pulse as a function of t_{p2} when $\omega_1 t_{p1} = 8.0$ and $\omega_1/\omega_Q = 2.0$ for both pulses. The 1Q coherence amplitude also contains the effect of the satellites. In this sense our results in Fig. 5 differ from those of Amoureux *et al.* (*14*), who considered only the transfer to the central transition $-\frac{1}{2} \leftrightarrow +\frac{1}{2}$. The

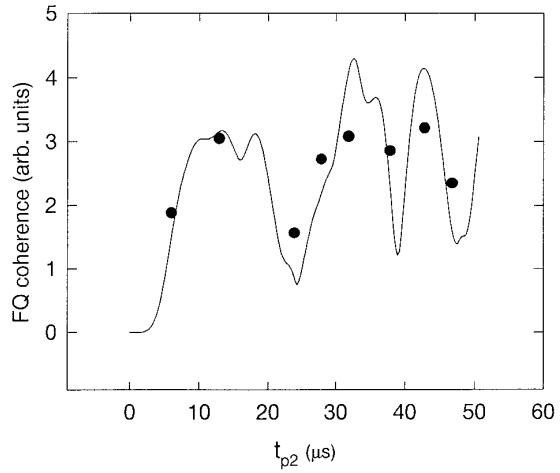

FIG. 5. FQ signal amplitude of ^{27}Al in Al_2O_3 versus t_{p2}. $t_{p1} = 40$ μs, $\omega_1 t_{p1} = 8.0$, $\tau_1 = 10$ μs, $\omega_Q/2\pi = 15.7$ kHz, and $\omega_1/\omega_Q = 2.0$ for both pulses.

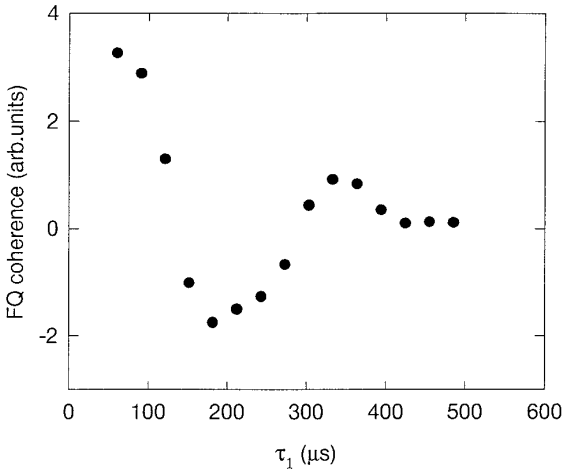

FIG. 6. Evolution of the FQ coherence during τ_1 at the resonance offset 3.37 kHz. $\omega_Q/2\pi = 15.7$ kHz, $\omega_1/\omega_Q = 2.0$, $\omega_1 t_{p1} = 8.0$, and $\omega_1 t_{p2} = 2.6$.

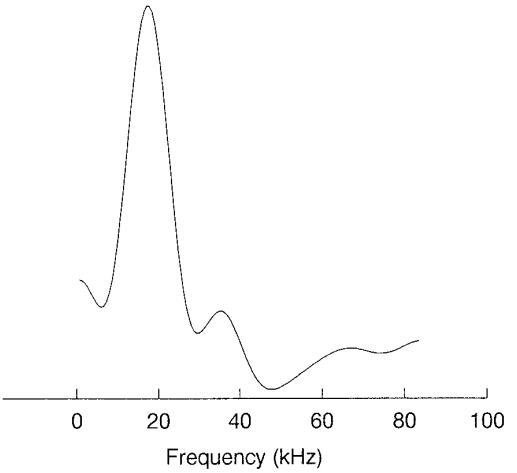

FIG. 7. FQ coherence spectrum calculated from the data of Fig. 6.

first maximum in Fig. 5 is obtained when $\omega_1 t_{p2} \cong 2.6$. The experimental points were obtained with the Al_2O_3 single crystal, oriented as explained above. Deviations of the experimental data from the theoretical calculations originate mainly from the rather wide 1Q lines in the spectrum (Fig. 2) and from the second order quadrupolar correction which were not included in the calculations. The second order correction does not broaden the $2I$ multiquantum coherence in single crystals but it has some effect on the evolution frequency.

The evolution of the 5Q coherence during the time τ_1 between the pulses was studied next. The optimum conditions were chosen for ω_1/ω_Q and the pulse lengths. The spectrometer frequency was shifted by 3.38 kHz relative to $\gamma B_0/2\pi$. The acquired signals after the two-pulse sequences were Fourier transformed relative to τ_2. The obtained amplitudes of the central resonance are shown in Fig. 6. When the Fourier transform of the experimental points of Fig. 6 was calculated relative to τ_1, the 5Q coherence spectrum of Fig. 7 was obtained. The spectral line occurs at about 16.5 kHz, or five times the resonance offset. The spectrum is in principle just a cross section of the two-dimensional spectrum parallel to the ω_1 axis.

It is interesting to consider the effect of the chemical shift, or equivalently of the heteronuclear dipolar interaction, on the excitation and detection of the 5Q coherence. This can be studied by introducing an offset $\Delta\omega$ for the RF irradiation. Our calculations show that the 5Q coherence excited by one RF pulse varies with $\Delta\omega/\omega_Q$, as described by the dashed curve in Fig. 8, when $\omega_1 t_{p1} = 8.0$ and $\omega_1/\omega_Q = 2.0$. The coherence amplitude decreases quite fast with the increasing offset. However, if we use a shorter pulse corresponding to the lower 5Q coherence maximum at $\omega_1 t_{p1} = 3.1$ in Figs. 3 and 4, the decrease is much slower, as shown by the solid curve in Fig. 8. The dotted curve in Fig. 8 represents the calculated variation of the 5Q coherence with $\Delta\omega/\omega_Q$ after phase-cycled two-pulse sequences, when $\omega_1 t_{p1} = 8.0$, $\omega_1 t_{p2} = 2.6$, and $\omega_1/\omega_Q = 2.0$. The second pulse causes an additional attenuation of the smaller maxima near $\Delta\omega/\omega_Q = \pm 0.8$, as can be seen by comparing the dashed and the dotted curves.

Finally we studied the effect of the pulse length on the intensity of the spectral lines after one RF pulse at the resonance frequency $\gamma B_0/2\pi$ for certain constant values of ω_1/ω_Q. In Figs. 9a–9c we represent the variation of the intensity ratio $R = I_c/I_s$ as a function of $\omega_Q t_p$ for $\omega_1/\omega_Q = 0.1$, $\omega_1/\omega_Q = 0.2$, and $\omega_1/\omega_Q = 0.5$, respectively. The quantities I_c and I_s are the intensities of the central and all the satellite lines. According to the linear response theory the satellite lines in the spectrum should vanish completely when $\omega_Q t_p = k\pi$ ($k = 1, 2, 3, \ldots$). For such pulse lengths the intensity ratio should grow very large, which behavior is qualitatively observed for $\omega_1/\omega_Q =$

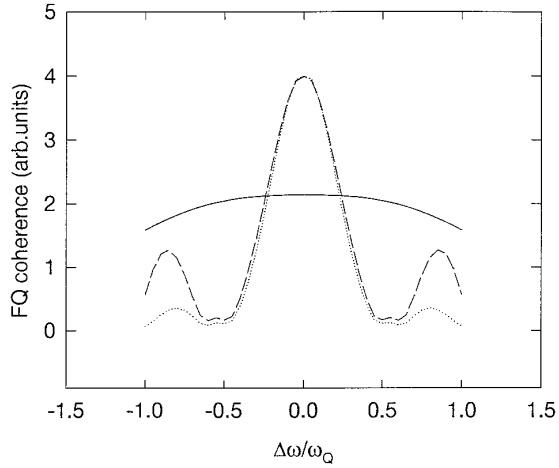

FIG. 8. Calculated variation of the FQ coherence amplitude versus the resonance offset $\Delta\omega$ during one RF pulse (dashed and solid curves with $\omega_1 t_{p1} = 8.0$ and 3.1, respectively) and during the two-pulse sequence (dotted curve with $\omega_1 t_{p1} = 8.0$ and $\omega_1 t_{p2} = 2.6$) for $\omega_1/\omega_Q = 2$.

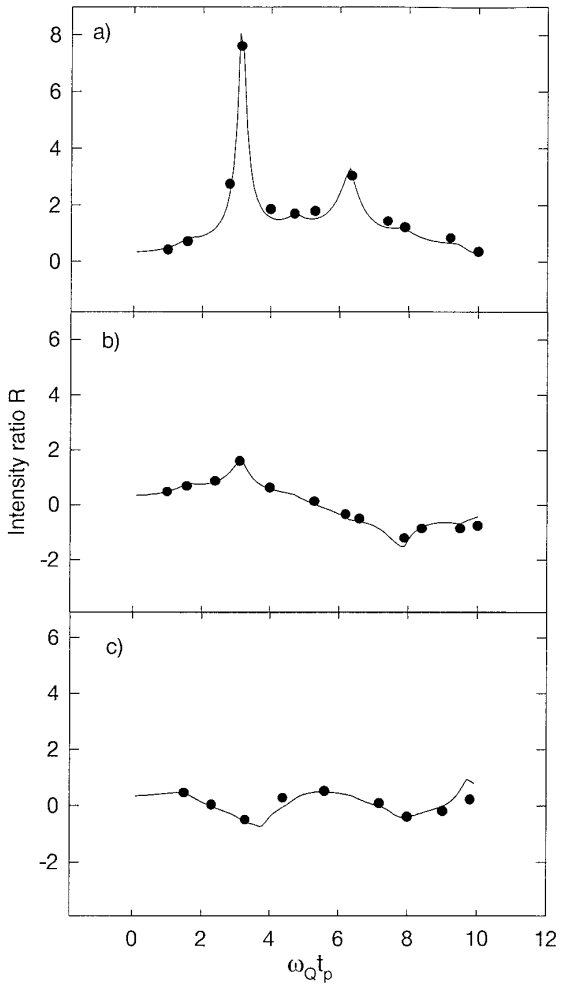

FIG. 9. Intensity ratio $R = I_c/I_s$ versus $\omega_Q t_p$ for $\omega_1/\omega_Q = 0.1$ (a), $\omega_1/\omega_Q = 0.2$ (b), and $\omega_1/\omega_Q = 0.5$ (c) after one pulse at $\omega_r = \gamma B_0$.

0.1 and to a smaller extent for $\omega_1/\omega_Q = 0.2$, but for $\omega_1/\omega_Q = 0.5$ no trace of such maxima can be found. This is a clear indication that the system of the quadrupolar spins $\frac{5}{2}$ cannot be treated as linear when the flip angle $\omega_1 t_p > \pi/10$. Obvious explanations for the deviation of the experimental data from theoretical curves are the finite width of the spectral lines, the second order quadrupolar effects, and pulse imperfections.

In conclusion we emphasize that multiquantum excitation and conversion back to an observable signal are most effective in samples with a relatively low quadrupole coupling, that is, $\omega_1 \geq \omega_Q$. As long as the quadrupole frequency is less than 300 kHz, multiquantum line widths similar to those of the single crystal absorption spectrum can be obtained even in polycrystalline samples without spinning. For larger quadrupole couplings when the second order correction dominates the line width, some sample spinning technique is unavoidable.

REFERENCES

1. S. Yatsiv, *Phys. Rev.* **113,** 1522 (1959).
2. R. R. Ernst, G. Bodenhausen, and A. Wokaun, ''Principles of Nuclear Magnetic Resonance in One and Two Dimensions,'' Claredon Press, Oxford (1987).
3. S. Vega and A. Pines, *J. Chem. Phys.* **66,** 5624 (1977).
4. D. Sandstrom and M. H. Levitt, *J. Am. Chem. Soc.* **118,** 6966 (1996).
5. D. E. Demco, S. Hafner, I. Ardeleanu, and R. Kimmich, *Appl. Magn. Reson.* **9,** 491 (1995).
6. K. Schmidt-Rohr, *Macromolecules* **29,** 3975 (1996).
7. P. P. Man, *J. Magn. Reson.* **94,** 258 (1991).
8. C. A. Fyfe, K. C. Wongmoon, Y. Huang, and H. Grondey, *Microporous Mater.* **5,** 29 (1995).
9. A. Samoson, E. Lippmaa, and A. Pines, *Mol. Phys.* **65,** 1013 (1988).
10. A. Llor and J. Virlet, *Chem. Phys. Lett.* **152,** 248 (1988).
11. B. F. Chmelka, K. T. Mueller, A. Pines, J. Stebbins, Y. Wu, and J. W. Zwanziger, *Nature* **339,** 42 (1989).
12. L. Frydman and J. S. Harwood, *J. Am. Chem. Soc.* **117,** 5367 (1995).
13. A. Medek, J. S. Harwood, and L. Frydman, *J. Am. Chem. Soc.* **117,** 12779 (1995).
14. J. P. Amoureux, C. Fernandez, and L. Frydman, *Chem. Phys. Lett.* **259,** 347 (1996).
15. C. Jäger, K. Herzog, B. Thomas, M. Feike, and G. Kunath-Fandrei, *Solid State NMR* **5,** 51 (1995).
16. C. Fernandez and J. P. Amoureux, *Solid State NMR* **5,** 315 (1996).
17. G. Wu, D. Rovnyak, B. Sun, and R. G. Griffin, *Chem. Phys. Lett.* **249,** 210 (1995).
18. D. Massiot, B. Touzo, D. Trumeau, J. P. Coutures, J. Virlet, P. Florian, and P. J. Grandinetti, *Solid State NMR* **6,** 73 (1996).
19. S. P. Brown, S. J. Heyes, and S. Wimperis, *J. Magn. Reson.* **119,** 280 (1996).
20. S. P. Brown and S. Wimperis, *J. Magn. Reson.* **128,** 42 (1997).
21. A. A. Maudsley, A. Wokaun, and R. R. Ernst, *Chem. Phys. Lett.* **55,** 9 (1978).
22. R. E. Hurd, *J. Magn. Reson.* **87,** 422 (1990).
23. L. Mitschang, H. Ponstingl, D. Grindrod, and H. Oschkinat, *J. Chem. Phys.* **102,** 3089 (1995).
24. P. B. Kingsley, *J. Magn. Reson. B* **109,** 243 (1995).
25. R. V. Pound, *Phys. Rev.* **79,** 685 (1950).
26. A. Wokaun and R. R. Ernst, *J. Chem. Phys.* **67,** 1752 (1977).
27. S. Vega, *J. Chem. Phys.* **68,** 5518 (1978).